

# Motion Control for Robotic Arm with Rotational Counterweights

Ryosuke Ishine<sup>1</sup>, Akihiro Kawamura<sup>2</sup>, Ryo Kurazume<sup>2</sup> and Sadao Kawamura<sup>3</sup>

**Abstract**—This paper proposes a new control method for the robotic arm with rotational counterweights. This robotic arm is actuated by gravitational and inertia torque of the counterweights. To date, the control law which achieves the angle control of the robot has been proposed. However, in the research, only 1 DOF robot is discussed. Moreover, the stability analysis of the dynamics hasn't been shown. The new control method proposed in this paper achieves the angle control of 2 DOFs, and we can prove the dynamic stability. In this paper, we show the convergence of the dynamics considering the method. Also we conduct numerical simulations for position control of 2 DOFs robotic arm. Verifying the angles of the robotic arm converge to its desired angles, the utility of the method is demonstrated.

## I. INTRODUCTION

Conventional robotic arms have been made of metal to increase their stiffness and precision of motion. However, it also causes a problem that the robots become heavy. In order to drive heavy joints and compensate their gravity effects, motors with high reduction gears have to be embedded in joints. The geared motors lead large friction effects on joints and decrease backdrivability. These problems have been discussed by a number of researchers so far.

In general, the solution is gravity compensation mechanism. Spring is one of the most popular structures for gravity compensation [1]–[3]. This structure can achieve the function without large weight gains though the structure becomes complicated. On the other hand, counterweight also works as gravity compensation [4], [5]. This structure is very simple though the total weight of robot system increases as shown in Figure 1 (A). In addition, this counterweight system makes the center of gravity approach the base of robots. This feature indicates the possibility to make the base of the robot arm light and slender. It is useful in narrow environment such as on vehicles. In this paper, we focus on the advantages of counterweight systems.

In order to enhance the feature of counterweights for gravity compensation, Akihiro *et al.* have proposed a robotic arm with a rotational counterweight [6]. In this system, the counterweight works as not only gravity compensation but also actuation. The gravitational equilibrium angle is shifted

<sup>1</sup> Ryosuke Ishine is with the Graduate School of Information Science and Electrical Engineering, Kyushu University, 744, Motoooka, Nishi-ku, Fukuoka, 8190395, JAPAN [ishine@irvs.ait.kyushu-u.ac.jp](mailto:ishine@irvs.ait.kyushu-u.ac.jp)

<sup>2</sup> Akihiro Kawamura and Ryo Kurazume are with the Faculty of Information Science and Electrical Engineering, Kyushu University, 744, Motoooka, Nishi-ku, Fukuoka, 8190395, JAPAN {[kawamura](mailto:kawamura@ait.kyushu-u.ac.jp), [@ait.kyushu-u.ac.jp](mailto:kurazume)}

<sup>3</sup> Sadao Kawamura is with Department of Robotics, Faculty of Science and Engineering, Ritsumeikan University, 1-1-1, Nojihigashi, Kusatsu-shi, Shiga, 5258577, JAPAN [kawamura@se.ritsumei.ac.jp](mailto:kawamura@se.ritsumei.ac.jp)

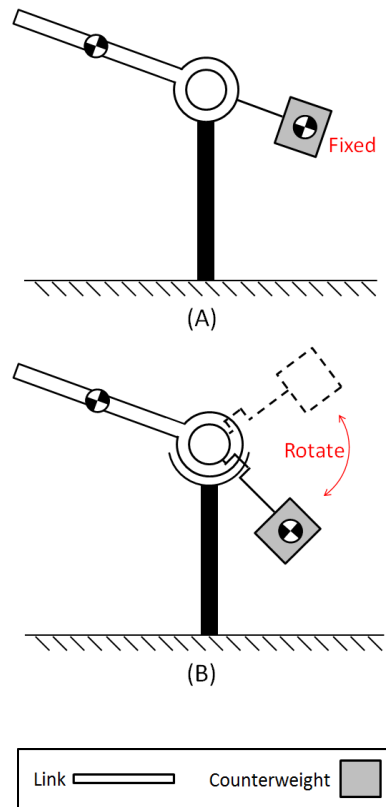


Fig. 1. (A)Fixed counterweight, (B)Rotational counterweight

by rotating the counterweight on the link. Then, the robot is driven to realize the angle. Figure 1 (B) shows the rotational counterweight structure. As shown in Figure 1 (B), a motor is not located in the joint. Then, the friction effect caused by reduction gears is reduced. Thereby, this system has high backdrivability. In terms of a robotic arm which has free joints, Torque Unit Manipulator (TUM) has been proposed [7]. In TUM, "torque units" are attached on an arbitrary place of the arm links. Torques generated by "torque units" actuate these links. However, in [7], the effect of gravitational force is not considered. Moreover, in the previous research [6], only 1 DOF robot is discussed and the stability analysis of the dynamics hasn't been shown.

In this paper, a new control method for the robotic arm with the rotational counterweights is proposed. In this method, the stability analysis of whole dynamics considering the controller is verified. In addition, it is applicable to 2 DOFs systems. The elicitation process of the analysis is formulated by referring to a research which proposes a controller for other underactuated system [8]. In what

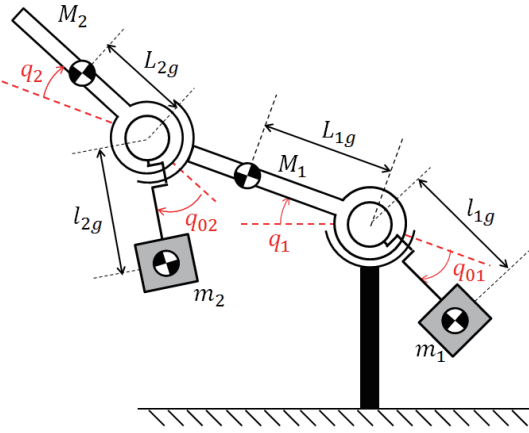


Fig. 2. The model of a robotic arm using rotational counterweights



Fig. 3. Real robotic arm using rotational counterweights

follows, section II shows the dynamics and the structure of the robot. In section III and IV, the new controller is proposed, and the stability analysis is done. Then, the results of numerical simulations using the controller is shown in section V.

## II. SYSTEM DESIGN

In this section, 2 DOFs robotic arm with rotational counterweights is introduced. Figures 2 and 3 show the model of the arm and the real robotic arm, respectively. The movable counterweights are installed and rotate on the links. Therefore, the joints between links do not have any actuators. It means that these joints are free. Most of the friction effects caused by geared motors on the joints are removed since there exists only bearings to connect links. The arm is driven by the inertia and gravitational forces generated by the counterweights.

As shown in Figure 2, the angle of the first link and the angle of the first counterweight relative to the first link are  $q_1$  and  $q_{01}$ , respectively. In a similar way, the angle of the second link relative to the first link and the angle of the second counterweight relative to the second link are  $q_2$  and  $q_{02}$ , respectively. The masses of the first and second links are denoted by  $M_1$  and  $M_2$ . Also, those of the counterweights are denoted by  $m_1$  and  $m_2$ . The distances toward the center of mass from the joints are denoted by  $L_{1g}$  and  $L_{2g}$ . Also, those of the counterweights are denoted by  $l_{1g}$  and  $l_{2g}$ .

Firstly, a vector of angles is defined as

$$\mathbf{q} = (q_1, q_2, q_{01}, q_{02})^T. \quad (1)$$

Then, the dynamics of this robotic arm is expressed as

$$\mathbf{H}\ddot{\mathbf{q}} + \mathbf{C} + \mathbf{G} = \boldsymbol{\tau}. \quad (2)$$

In (2),  $\mathbf{H}$  is  $4 \times 4$  matrix and

$$\mathbf{C} = (C_1, C_2, C_{01}, C_{02})^T, \quad (3)$$

$$\mathbf{G} = (G_1, G_2, G_{01}, G_{02})^T, \quad (4)$$

$$\boldsymbol{\tau} = (0, 0, \tau_{01}, \tau_{02})^T, \quad (5)$$

$$\begin{aligned} H_{11} = & M_1 L_{1g}^2 + M_2 L_{2g}^2 + m_1 l_{1g}^2 + m_2 l_{2g}^2 \\ & + M_2 L_1^2 + m_2 L_1^2 + 2M_2 L_1 L_{2g} \cos q_2 \\ & - 2m_2 L_1 l_{2g} \cos(q_2 + q_{02}), \end{aligned} \quad (6)$$

$$\begin{aligned} H_{12} = & H_{21} = M_2 L_{2g}^2 + m_2 l_{2g}^2 + M_2 L_1 L_{2g} \cos q_2 \\ & - m_2 L_1 l_{2g} \cos(q_2 + q_{02}) \end{aligned} \quad (7)$$

$$H_{13} = H_{31} = H_{33} = m_1 l_{1g}^2 \quad (8)$$

$$H_{14} = H_{41} = m_2 l_{2g}^2 - m_2 L_1 l_{2g} \cos(q_2 + q_{02}) \quad (9)$$

$$H_{22} = M_2 L_{2g}^2 + m_2 l_{2g}^2 \quad (10)$$

$$H_{24} = H_{42} = m_2 l_{2g}^2 \quad (11)$$

$$H_{44} = m_2 l_{2g}^2 \quad (12)$$

$$H_{23} = H_{32} = H_{34} = H_{43} = 0 \quad (13)$$

$$\begin{aligned} C_1 = & -M_2 L_1 L_{2g} (2\dot{q}_1 + \dot{q}_2) \dot{q}_2 \sin q_2 \\ & + m_2 L_1 l_{2g} (2\dot{q}_1 + \dot{q}_2 + \dot{q}_{02}) (\dot{q}_2 + \dot{q}_{02}) \\ & \sin(q_2 + q_{02}) \end{aligned} \quad (14)$$

$$\begin{aligned} C_2 = & M_2 L_1 L_{2g} \dot{q}_1^2 \sin q_2 \\ & - m_2 L_1 l_{2g} \dot{q}_1^2 \sin(q_2 + q_{02}) \end{aligned} \quad (15)$$

$$C_{01} = 0 \quad (16)$$

$$C_{02} = -m_2 L_1 l_{2g} \dot{q}_1^2 \sin(q_2 + q_{02}) \quad (17)$$

$$\begin{aligned} G_1 = & (M_1 L_{1g} + M_2 L_1 + m_2 L_1) g \cos q_1 \\ & + M_2 g L_{2g} \cos(q_1 + q_2) - m_1 g l_{1g} \cos(q_1 + q_{01}) \\ & - m_2 g l_{2g} \cos(q_1 + q_2 + q_{02}) \end{aligned} \quad (18)$$

$$\begin{aligned} G_2 = & M_2 g L_{2g} \cos(q_1 + q_2) \\ & - m_2 g l_{2g} \cos(q_1 + q_2 + q_{02}) \end{aligned} \quad (19)$$

$$G_{01} = -m_1 g l_{1g} \cos(q_1 + q_{01}) \quad (20)$$

$$G_{02} = -m_2 g l_{2g} \cos(q_1 + q_2 + q_{02}) \quad (21)$$

$\mathbf{H}$  denotes the inertia matrix of the robot.  $\mathbf{C}$  is the vector represents coriolis and centrifugal force of the robot.  $\mathbf{G}$  expresses gravity terms of the arm links and the counterweights. The symbol  $\boldsymbol{\tau}$  represents the input torques of the motors mounted on the arm links which actuate the counterweights. The input torques are shown in only the dynamics of the counterweights side in (5) since this system is an underactuated system.

### III. CONTROL LAW

In this section, we show a new control method for the robotic arm. In general, it has been difficult to control underactuated system stably. In the most of the researches about underactuated system, inverted pendulums has been discussed. Thereby, we have to develop a new control method for the arm with the rotational counterweights since the dynamic model is different. To date, a control law has been proposed for the rotational counterweight robot by Akihiro *et al.* [6]. The angle control of the robot is achieved by using this control law. However, the convergence of the closed-loop dynamics is not verified and only 1 DOF robot arm has been discussed. Therefore, it is difficult to apply to multi DOFs robot and to discuss about stability region of the desired angle and the coefficients in the method.

In this paper, a new control method is proposed in which the dynamic stability is proven. Also, it is applicable to the 2 DOFs robot. The method is based on the previous work [6] and refers to an elicitation process to satisfy a stability analysis which has been proposed by Chun *et al.* [9]. The proposed method is obtained as follows:

$$\tau_{01} = -K_{p1}(q_{1d} - q_1) + K_{v1}\dot{q}_1 - K_{v01}\dot{q}_{01} - \tau_{c1} - (M_1L_{1g} + M_2L_1 + m_2L_1)g \cos q_1 \quad (22)$$

$$\tau_{02} = -K_{p2}(q_{2d} - q_2) + K_{v2}\dot{q}_2 - K_{v02}\dot{q}_{02} - M_2gL_{2g} \cos(q_1 + q_2) - \tau_{c2} \quad (23)$$

$$\tau_{c1} = \frac{(1+k_1)\dot{q}_{01}}{\dot{q}_{01}^2 + \delta_1} [(\dot{q}_1 + \dot{q}_{01})\tau_{d11} + \dot{q}_1\tau_{d12}] \quad (24)$$

$$\tau_{c2} = \frac{(1+k_2)\dot{q}_{02}}{\dot{q}_{02}^2 + \delta_2} (\dot{q}_2 + \dot{q}_{02})\tau_{d2} \quad (25)$$

$$\tau_{d11} = -K_{p1}(q_{1d} - q_1) + K_{v1}\dot{q}_1 + m_1gl_{1g} \cos(q_1 + q_{01}) - (M_1L_{1g} + M_2L_1 + m_2L_1)g \cos q_1 \quad (26)$$

$$\tau_{d12} = m_2gl_{2g} \cos(q_1 + q_2 + q_{02}) - M_2gL_{2g} \cos(q_1 + q_2) \quad (27)$$

$$\tau_{d2} = -K_{p2}(q_{2d} - q_2) + K_{v2}\dot{q}_2 + m_2gl_{2g} \cos(q_1 + q_2 + q_{02}) - M_2gL_{2g} \cos(q_1 + q_2) \quad (28)$$

$$\dot{k}_1 = \begin{cases} \frac{\eta_1}{k_1} \left( \frac{k_1\dot{q}_{01}^2 - \delta_1}{\dot{q}_{01}^2 + \delta_1} \right) & (k_1 \neq 0) \\ \delta_1 & (k_1 = 0) \end{cases} \quad (29)$$

$$\dot{k}_2 = \begin{cases} \frac{\eta_2}{k_2} \left( \frac{k_2\dot{q}_{02}^2 - \delta_2}{\dot{q}_{02}^2 + \delta_2} \right) (\dot{q}_2 + \dot{q}_{02})\tau_{d2} & (k_2 \neq 0) \\ \delta_2 & (k_2 = 0) \end{cases} \quad (30)$$

where  $K_{p1}$ ,  $K_{p2}$ ,  $K_{v1}$ ,  $K_{v2}$ ,  $K_{v01}$ ,  $K_{v02}$ ,  $\delta_1$ ,  $\delta_2$ ,  $\eta_1$  and  $\eta_2$  are positive constants. The symbol  $q_{1d}$  and  $q_{2d}$  represent desired angles of the first and second links, respectively.  $K_{v1}\dot{q}_1$  and  $K_{v2}\dot{q}_2$  are dumping terms of the first and second links. Similarly,  $K_{v01}\dot{q}_{01}$  and  $K_{v02}\dot{q}_{02}$  are those of the counterweights. In this method,  $\tau_{c1}$  and  $\tau_{c2}$  are in the sense of [9]. By adding these terms, we can get the stability of whole dynamics. The symbol  $k_1$   $k_2$  are the adaptive terms.

In other words, this control method is designed in order to show the stability analysis of whole dynamics.

### IV. STABILITY ANALYSIS

In this section, the stability analysis of the dynamics considering the proposed method is shown. From (2), we can obtain

$$\mathbf{H}\ddot{\mathbf{q}} + \left( \frac{1}{2}\dot{\mathbf{H}} + \mathbf{S} \right) \dot{\mathbf{q}} + \mathbf{G} = \boldsymbol{\tau}. \quad (31)$$

In (31),  $\dot{\mathbf{H}}$  is the time differential matrix of the inertia matrix and  $\mathbf{S}$  is the  $4 \times 4$  skew-symmetric matrix. Some components of the matrix  $\mathbf{S}$  are expressed as follows:

$$S_{12} = -\frac{1}{2}M_2L_1L_{2g}(2\dot{q}_1 + \dot{q}_2) \sin q_2 + \frac{1}{2}m_2L_1l_{2g}(2\dot{q}_1 + \dot{q}_2 + \dot{q}_{02}) \sin(q_2 + q_{02}), \quad (32)$$

$$S_{14} = \frac{1}{2}m_2L_1l_{2g}(2\dot{q}_1 + \dot{q}_2 + \dot{q}_{02}) \sin(q_2 + q_{02}) \quad (33)$$

$$S_{21} = -S_{12}, \quad (34)$$

$$S_{41} = -S_{14}, \quad (35)$$

and the others are equal to zero.

By taking a sum of inner product of (31) and time differential of (1), the closed loop dynamics expressed as

$$\dot{\mathbf{q}}^T \mathbf{H} \ddot{\mathbf{q}} + \dot{\mathbf{q}}^T \left( \frac{1}{2} \dot{\mathbf{H}} + \mathbf{S} \right) \dot{\mathbf{q}} - \dot{\mathbf{q}}^T (-\mathbf{G} + \boldsymbol{\tau}) = \mathbf{0} \quad (36)$$

Then, the first and second terms of (31) is rearranged as follows:

$$\begin{aligned} \dot{\mathbf{q}}^T \mathbf{H} \ddot{\mathbf{q}} + \frac{1}{2} \dot{\mathbf{q}}^T \dot{\mathbf{H}} \dot{\mathbf{q}} + \dot{\mathbf{q}}^T \mathbf{S} \dot{\mathbf{q}} \\ = \frac{d}{dt} \left[ \frac{1}{2} \dot{\mathbf{q}}^T \mathbf{H} \dot{\mathbf{q}} \right] + \dot{\mathbf{q}}^T \mathbf{S} \dot{\mathbf{q}}. \end{aligned} \quad (37)$$

Since  $\mathbf{S}$  is the skew-symmetric matrix, we can obtain

$$\dot{\mathbf{q}}^T \mathbf{S} \dot{\mathbf{q}} = \mathbf{0}. \quad (38)$$

The third term of (31) is rearranged as follows:

$$\dot{\mathbf{q}}^T (-\mathbf{G} + \boldsymbol{\tau}) = -\dot{\mathbf{q}}^T \mathbf{G} + \dot{q}_{01}\tau_{01} + \dot{q}_{02}\tau_{02} \quad (39)$$

The second term of (39) is rearranged as follows:

$$\begin{aligned} \dot{q}_{01}\tau_{01} &= (\dot{q}_1 + \dot{q}_{01})\tau_{d11} + \dot{q}_1\tau_{d12} - K_{v1}\dot{q}_1^2 - K_{v01}\dot{q}_{01}^2 \\ &\quad - \dot{q}_{01}\tau_{c1} - \frac{d}{dt} \left[ \frac{1}{2} K_{p1} (q_{1d} - q_1)^2 \right] \\ &\quad + \dot{q}_1 G_1 + \dot{q}_{01} G_{01} \end{aligned} \quad (40)$$

The third term of (39) is rearranged as follows:

$$\begin{aligned} \dot{q}_{02}\tau_{02} &= (\dot{q}_2 + \dot{q}_{02})\tau_{d2} - K_{v2}\dot{q}_2^2 - K_{v02}\dot{q}_{02}^2 \\ &\quad - \dot{q}_{02}\tau_{c2} - \frac{d}{dt} \left[ \frac{1}{2} K_{p2} (q_{2d} - q_2)^2 \right] \\ &\quad + \dot{q}_2 G_2 + \dot{q}_{02} G_{02} \end{aligned} \quad (41)$$

In addition, if  $k_1$  and  $k_2$  are not equal to zero, (29) and (30) can be written as follows:

$$\begin{aligned} \frac{k_1 \dot{q}_{01}^2}{\dot{q}_{01}^2 + \delta_1} [(\dot{q}_1 + \dot{q}_{01}) \tau_{d11} + \dot{q}_1 \tau_{d12}] \\ = \frac{k_1 \dot{k}_1}{\eta_1} + \frac{\delta_1}{\dot{q}_{01}^2 + \delta_1} [(\dot{q}_1 + \dot{q}_{01}) \tau_{d11} + \dot{q}_1 \tau_{d12}]. \end{aligned} \quad (42)$$

$$\begin{aligned} \frac{k_2 \dot{q}_{02}^2}{\dot{q}_{02}^2 + \delta_2} (\dot{q}_2 + \dot{q}_{02}) \tau_{d2} \\ = \frac{k_2 \dot{k}_2}{\eta_2} + \frac{\delta_2}{\dot{q}_{02}^2 + \delta_2} (\dot{q}_2 + \dot{q}_{02}) \tau_{d2}. \end{aligned} \quad (43)$$

These expressions are based on the sense of [9]. Therefore,

$$\dot{q}_{01} \tau_{c1} = \frac{d}{dt} \left[ \frac{k_1^2}{2\eta_1} \right] + (\dot{q}_1 + \dot{q}_{01}) \tau_{d11} + \dot{q}_1 \tau_{d12}. \quad (44)$$

$$\dot{q}_{02} \tau_{c2} = \frac{d}{dt} \left[ \frac{k_2^2}{2\eta_2} \right] + (\dot{q}_2 + \dot{q}_{02}) \tau_{d2}. \quad (45)$$

By substituting (44) into (40), we obtain

$$\begin{aligned} \dot{q}_{01} \tau_{01} = & -\frac{d}{dt} \left[ \frac{1}{2} K_{p1} (q_{1d} - q_1)^2 + \frac{k_1^2}{2\eta_1} \right] \\ & - K_{v1} \dot{q}_1^2 - K_{v01} \dot{q}_{01}^2 + \dot{q}_1 G_1 + \dot{q}_{01} G_{01} \end{aligned} \quad (46)$$

From (41) and (45),

$$\begin{aligned} \dot{q}_{02} \tau_{02} = & -\frac{d}{dt} \left[ \frac{1}{2} K_{p2} (q_{2d} - q_2)^2 + \frac{k_2^2}{2\eta_2} \right] \\ & - K_{v2} \dot{q}_2^2 - K_{v02} \dot{q}_{02}^2 + \dot{q}_2 G_2 + \dot{q}_{02} G_{02} \end{aligned} \quad (47)$$

By substituting (46) and (47) into (39), we obtain

$$\begin{aligned} \dot{\mathbf{q}}^T (-\mathbf{G} + \boldsymbol{\tau}) = & -K_{v1} \dot{q}_1^2 - K_{v01} \dot{q}_{01}^2 - K_{v2} \dot{q}_2^2 - K_{v02} \dot{q}_{02}^2 \\ & - \frac{d}{dt} \left[ \frac{1}{2} K_{p1} (q_{1d} - q_1)^2 + \frac{k_1^2}{2\eta_1} \right. \\ & \left. + \frac{1}{2} K_{p2} (q_{2d} - q_2)^2 + \frac{k_2^2}{2\eta_2} \right] \end{aligned} \quad (48)$$

From (37) and (48),

$$\begin{aligned} \frac{d}{dt} \left[ \frac{1}{2} \dot{\mathbf{q}}^T \mathbf{H} \dot{\mathbf{q}} + \frac{1}{2} K_{p1} (q_{1d} - q_1)^2 \right. \\ \left. + \frac{1}{2} K_{p2} (q_{2d} - q_2)^2 + \frac{k_1^2}{2\eta_1} + \frac{k_2^2}{2\eta_2} \right] \\ = -K_{v1} \dot{q}_1^2 - K_{v01} \dot{q}_{01}^2 - K_{v2} \dot{q}_2^2 - K_{v02} \dot{q}_{02}^2. \end{aligned} \quad (49)$$

Therefore, if we consider the positive function  $V$ ,

$$\begin{aligned} V = & \frac{1}{2} \dot{\mathbf{q}}^T \mathbf{H} \dot{\mathbf{q}} + \frac{1}{2} K_{p1} (q_{1d} - q_1)^2 \\ & + \frac{1}{2} K_{p2} (q_{2d} - q_2)^2 + \frac{k_1^2}{2\eta_1} + \frac{k_2^2}{2\eta_2}, \end{aligned} \quad (50)$$

and

$$\begin{aligned} \dot{V} = & -K_{v1} \dot{q}_1^2 - K_{v01} \dot{q}_{01}^2 - K_{v2} \dot{q}_2^2 - K_{v02} \dot{q}_{02}^2 \\ \leq & 0, \end{aligned} \quad (51)$$

TABLE I  
PHYSICAL PARAMETERS

Link length	$L_1$	0.20 [m]
	$L_2$	0.20 [m]
Counterweight length	$l_1$	0.15 [m]
	$l_2$	0.15 [m]
Center of mass of link	$L_{1g}$	0.09 [m]
	$L_{2g}$	0.09 [m]
Center of mass of counterweight	$l_{1g}$	0.07 [m]
	$l_{2g}$	0.07 [m]
Link mass	$M_1$	0.20 [kg]
	$M_2$	0.20 [kg]
Counterweight mass	$m_1$	5.0 [kg]
	$m_2$	0.80 [kg]

TABLE II  
CONTROLLER PARAMETERS

$K_p$	0.10
$K_{v1}$	0.20
$K_{v2}$	0.02
$J_p$	0.10
$J_{v1}$	0.10
$J_{v2}$	0.05
$\delta_1$	0.002
$\delta_2$	0.002
$\eta_1$	0.000001
$\eta_2$	0.000001

TABLE III  
INITIAL CONDITION

$\dot{q}_1$	0.00 [rad/s]
$\dot{q}_2$	0.00 [rad/s]
$\dot{q}_{01}$	0.00 [rad/s]
$\dot{q}_{02}$	0.00 [rad/s]
$q_1$	-1.57 [rad]
$q_2$	0.00 [rad]
$q_{01}$	3.14 [rad]
$q_{02}$	3.14 [rad]

are obtained. Equations (50) and (51) yield

$$\begin{aligned} \int_0^\infty (-K_{v1} \dot{q}_1^2 - K_{v01} \dot{q}_{01}^2 - K_{v2} \dot{q}_2^2 - K_{v02} \dot{q}_{02}^2) dt \\ \leq V(0) - V(t) \leq V(0), \end{aligned} \quad (52)$$

This equation shows that the joint angle velocities  $\dot{q}_1(t)$ ,  $\dot{q}_2(t)$ ,  $\dot{q}_{01}(t)$  and  $\dot{q}_{02}(t)$  are squared integrable over time  $t \in (0, \infty)$ . It shows that  $\dot{q}_1(t)$ ,  $\dot{q}_2(t)$ ,  $\dot{q}_{01}(t)$ ,  $\dot{q}_{02}(t) \in L^2(0, \infty)$ . Thereby, the output of the overall system  $\dot{\mathbf{q}}(t)$  is uniformly continuous since it is shown that  $\dot{\mathbf{q}} \rightarrow 0$  and  $\ddot{\mathbf{q}} \rightarrow 0$  if  $t \rightarrow \infty$  [8]. Therefore, it is clear that the joint angle  $q_1$  and  $q_2$  converge to their desired angles  $q_{1d}$  and  $q_{2d}$  from (50), respectively.

## V. NUMERICAL SIMULATIONS

Several numerical simulations to show the effectiveness of the proposed method are conducted here. The simulator is developed using the dynamics shown in (2). The physical parameters of the robot are shown in Table I. Table II shows the parameters in (22)-(30). The initial condition of the robot arm is shown in Table III. In initial state, the arm links and the counterweights are vertically downward (Figure 4 (A)).

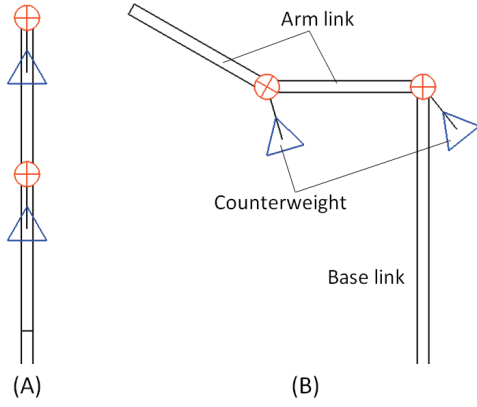


Fig. 4. (A) Initial state of simulations. (B) One of desired states of simulations.

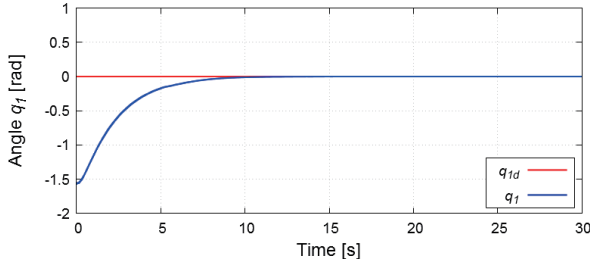


Fig. 5. The transient response of  $q_1$  when desired angles are  $q_{1d} = 0$  [rad] and  $q_{2d} = 0.52$  [rad].

In this paper, numerical simulations for two different desired angles  $q_{1d} = 0^\circ$ ,  $q_{2d} = 30^\circ$  and  $q_{1d} = 30^\circ$ ,  $q_{2d} = -30^\circ$  are conducted. Figures 5, 6, 7 and 8 show the transient responses of  $q_1$ ,  $q_2$ ,  $q_{01}$  and  $q_{02}$  respectively in the case where the desired angles are  $q_{1d} = 0^\circ$  and  $q_{2d} = 30^\circ$ . Furthermore, the transient of input torques  $\tau_{01}$ ,  $\tau_{02}$  are shown in Figures 9,10. Similarly, figures 11, 12, 13 and 14 show the transient responses of  $q_1$ ,  $q_2$ ,  $q_{01}$  and  $q_{02}$  respectively in the case where the desired angles are  $q_{1d} = 30^\circ$  and  $q_{2d} = -30^\circ$ . The transient of input torques  $\tau_{01}$ ,  $\tau_{02}$  in this case are shown in Figures 15,16. From these results, it is confirmed that the joint angles  $q_1$  and  $q_2$  converge to their desired value. Moreover, the angles of the counterweights  $q_{01}$  and  $q_{02}$  converge to constant values although we haven't set desired angles of counterweights. The constant values are equivalent to the equilibrium angles of counterweights to satisfy the following equations.

$$\begin{aligned} & (M_1 L_{1g} + M_2 L_1 + m_2 L_1) g \cos q_1 \\ & + M_2 g L_{2g} \cos(q_1 + q_2) - m_1 g l_{1g} \cos(q_1 + q_{01}) \\ & - m_2 g l_{2g} \cos(q_1 + q_2 + q_{02}) = 0, \end{aligned} \quad (53)$$

$$\begin{aligned} & M_2 g L_{2g} \cos(q_1 + q_2) \\ & - m_2 g l_{2g} \cos(q_1 + q_2 + q_{02}) = 0 \end{aligned} \quad (54)$$

Furthermore, input torques of counterweights  $\tau_{01}$ ,  $\tau_{02}$  also converge to constant values. Then, the usefulness of the proposed method and the dynamic stability are verified.

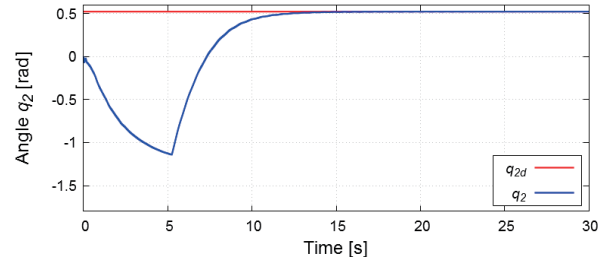


Fig. 6. The transient response of  $q_2$  when desired angles are  $q_{1d} = 0$  [rad] and  $q_{2d} = 0.52$  [rad].

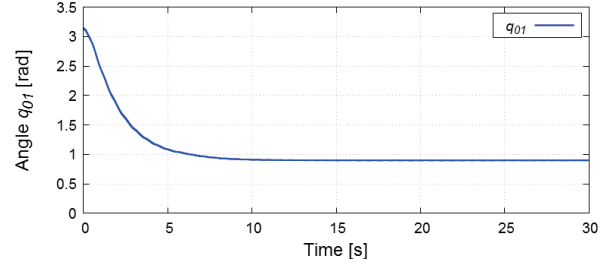


Fig. 7. The transient response of  $q_{01}$  when desired angles are  $q_{1d} = 0$  [rad] and  $q_{2d} = 0.52$  [rad].

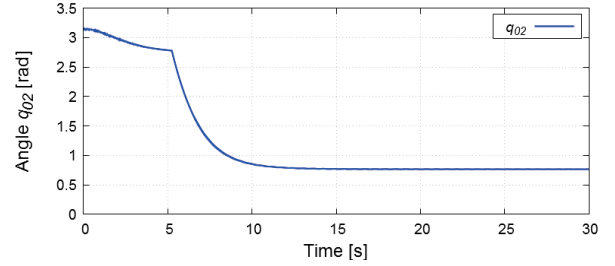


Fig. 8. The transient response of  $q_{02}$  when desired angles are  $q_{1d} = 0$  [rad] and  $q_{2d} = 0.52$  [rad].

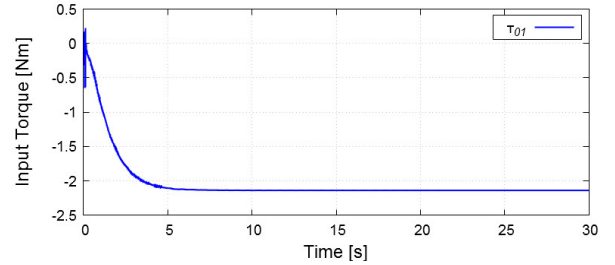


Fig. 9. The transient of  $\tau_{01}$  when desired angles are  $q_{1d} = 0$  [rad] and  $q_{2d} = 0.52$  [rad].

## VI. CONCLUSION

In this paper, we proposed a new control method for the rotational counterweight robot arm. Using this method, the convergences of the closed-loop dynamics and joint angles toward their desired angles are verified theoretically. Moreover, the effectiveness of the proposed method and the stability analysis are verified by the results of numerical simulations. In future works, experiments using real robotic arms must be conducted.

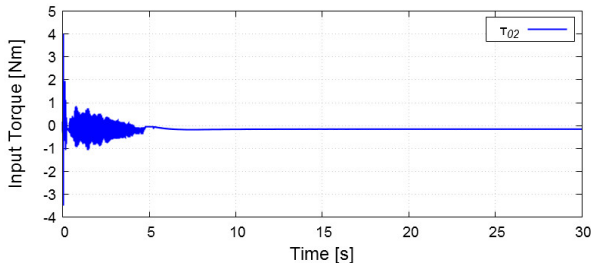


Fig. 10. The transient of  $\tau_{02}$  when desired angles are  $q_{1d} = 0$  [rad] and  $q_{2d} = 0.52$  [rad].

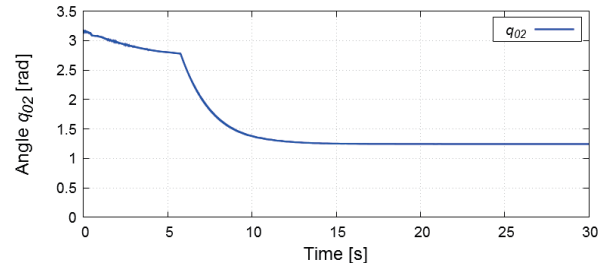


Fig. 14. The transient response of  $q_{02}$  when desired angles are  $q_{1d} = 0.52$  [rad] and  $q_{2d} = -0.52$  [rad].

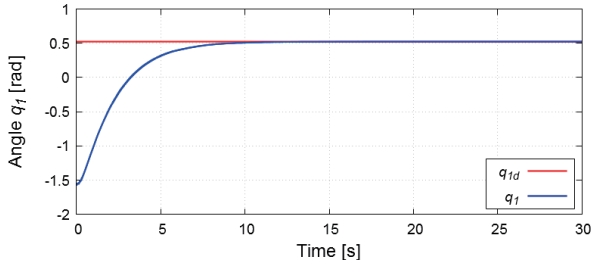


Fig. 11. The transient response of  $q_1$  when desired angles are  $q_{1d} = 0.52$  [rad] and  $q_{2d} = -0.52$  [rad].

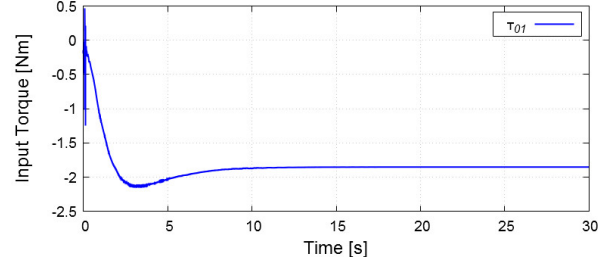


Fig. 15. The transient of  $\tau_{01}$  when desired angles are  $q_{1d} = 0.52$  [rad] and  $q_{2d} = -0.52$  [rad].

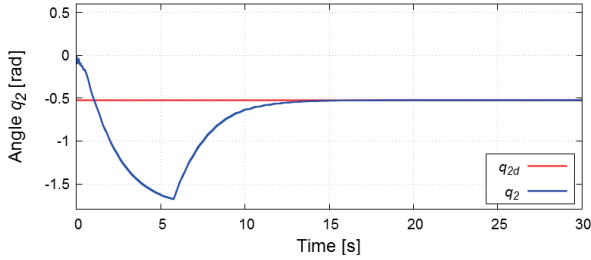


Fig. 12. The transient response of  $q_2$  when desired angles are  $q_{1d} = 0.52$  [rad] and  $q_{2d} = -0.52$  [rad].

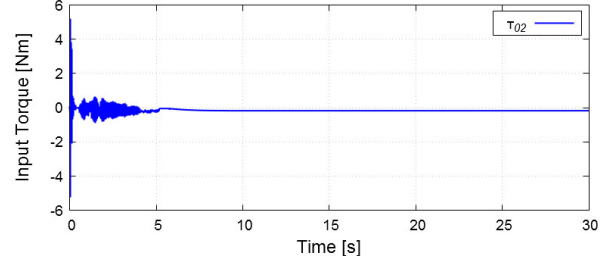


Fig. 16. The transient of  $\tau_{02}$  when desired angles are  $q_{1d} = 0.52$  [rad] and  $q_{2d} = -0.52$  [rad].

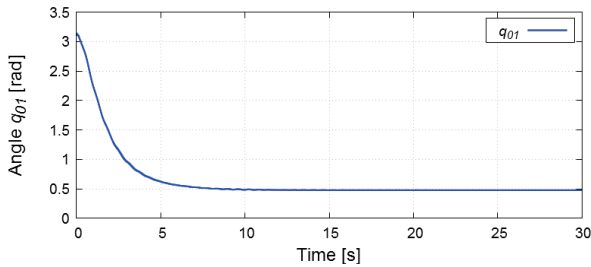


Fig. 13. The transient response of  $q_{01}$  when desired angles are  $q_{1d} = 0.52$  [rad] and  $q_{2d} = -0.52$  [rad].

## ACKNOWLEDGMENT

The present study was supported in part by a Grant-in-Aid for Young Scientists (B) (16K18053).

## REFERENCES

[1] G. Endo, H. Yamada, A. Yajima, M. Ogata and S. Hirose, "A passive weight compensation mechanism with a non-circular pulley and a spring," Proc. of the IEEE Int. Conf. on Robotics and Automation, pp. 3843-3848, 2010.

[2] A. Gopalswamy, P. Gupta and M. Vidyasagar, "A new parallelogram linkage configuration for gravity compensation using torsional springs," Proc. of the IEEE Int. Conf. on Robotics and Automation, pp. 664-669, 1992.

[3] Rogier Barents, Mark Schenk, Wouter D. van Dorsser, Boudewijn M. Wisse and Just L. Herder, "Spring-to-Spring Balancing as Energy-Free Adjustment Method in Gravity Equilibrators," Journal of Mechanical Design, 133(6), 2011

[4] Vigen Arakelian, Jean-Paul Le Baron and Pauline Mottu, "Torque minimisation of the 2-DOF serial manipulators based on minimum energy consideration and optimum mass redistribution," Mechatronics, 21 (1), pp. 310-314, 2011.

[5] J. P. Whitney and J. K. Hodgins, "A passively safe and gravity counterbalanced anthropomorphic robot arm," Proc. of the IEEE Int. Conf. on Robotics and Automation, pp. 6168-6173, HongKong, China, 2014.

[6] A. Kawamura, B. Gang, M. Uemura and S. Kawamura, "Mechanism and Control of Robotic Arm using Rotational Counterweights," Proc. of the IEEE Int. Conf. on Robotics and Automation (ICRA), pp. 2716-2721, 2015.

[7] K. Osuka, K. Yoshida and T. Ono, "New design concept of space manipulator: a proposal of Torque-unit Manipulator," Proc. of the IEEE Conf. on Decision and Control, pp. 1823-1825, 1994

[8] S. Arimoto, "A differential-geometric approach for 2-D and 3-D object grasping and manipulation," Annual Review in Control, Vol. 31, pp. 189-209, 2007.

[9] Chun-Yi Su and Yury Stepanenko, "Adaptive Variable Structure Set-Point Control of Underactuated Robots," IEEE Transactions on Automatic Control, 44(11), pp. 2090-2093, 1999.